ELSEVIER

Theoretical and Applied Fracture Mechanics 36 (2001) 147–164

theoretical and applied fracture mechanics

www.elsevier.com/locate/tafmec

Microscopic analysis of crack propagation for multiple cracks, inclusions and voids

I. Demir [a], H.M. Zbib [b,*], M. Khaleel [c]

[a] *Mechanical Engineering Department, King Saud University, P.O. Box 800, Riyadh 11421, Saudi Arabia*
[b] *School of Mechanical and Materials Engineering, Washington State University, P.O. Box 642920, Pullman, WA 99164-2920, USA*
[c] *Pacific Northwest National Laboratory, Richland, WA, USA*

Abstract

The elastic crack interaction with internal defects, such as microcracks, voids and rigid inclusions, is investigated in this study for the purpose of analyzing crack propagation. The elastic stress field is obtained using linear theory of elasticity for isotropic materials. The cracks are modeled as pile-ups of edge dislocations resulting into a coupled set of integral equations, whose kernels are those of a dislocation in a medium with or without an inclusion or void. The numerical solution of these equations gives the stress intensity factors and the complete stress field in the given domain. The solution is valid for a general solid, however the propagation analysis is valid mostly for brittle materials. Among different propagation models the ones based on maximum circumferential stress and minimum strain energy density theories, are employed. A special emphasis is given to the estimation of the crack propagation direction that defines the direction of crack branching or kinking. Once a propagation direction is determined, an improved model dealing with kinked cracks must be employed to follow the propagation behavior.

1. Introduction

Understanding failure and its driving mechanisms is very important for design engineers. It has been widely observed that small defects, voids and cracks are mainly responsible for the initiation of failure. Therefore it is very much desirable to understand the mechanical implications of these imperfections and to establish a technique to model the process of initiation and progress of failure. Propagation of cracks is a leading phenomenon in the fracture mechanics of brittle materials. While it can be thought of as being a major driving mechanism in the failure process, it can also provide a toughening mechanism through branching, kinking and propagation, as well as initiation of micro-cracks in all possible directions. Therefore, the analysis of crack growth, interaction and crack stability, has been a major subject in fracture mechanics research. There have been numerous studies since the early work of Griffith on the subject, concentrating on branching, curving and kinking of cracks in isotropic and anisotropic solids [1–5]. The major objective in most of these studies is to predict the conditions and path along which a crack propagates. Associated field variables and resulting fracture parameters can be obtained by using advanced computational techniques at each stage of propagation. Starting from a basic crack configuration, the

* Corresponding author. Tel.: +1-509-335-7832; fax: +1-509-335-4662.
E-mail address: zbib@mme.wsu.edu (H.M. Zbib).

0167-8442/01/$ - see front matter
PII: S0167-8442(01)00065-9

kinking, branching or propagation direction can be estimated based on some criteria. Depending on the material type, the most accurate propagation criteria can be chosen to estimate the propagation direction. It must be noted that there are studies proposing general formulation of crack path analysis in the form of displacement based boundary value problems [6]. These types of techniques are still in the development stage and may be used in the case of multiple cracks.

It is well known that different crack propagation direction theories do not agree well in some cases. The maximum circumferential stress theory, the minimum strain energy density theory and the maximum energy release rate theory are the most important and widely used ones among the theories on crack propagation. Among these three theories, the first two are employed in this study. The third one and its modified versions [7] that use G or J integral are not considered here since they are still surrounded with controversies. Especially in mixed mode conditions the performance of the theory is not very good. Moreover it is shown in [8] that the energy release rate (G) or J-integral could not yield the correct result of crack growth under electric field reversal. The shortcomings of G or J appear especially in multiscale problems.

The propagation theories require calculation of the entire stress field. Therefore, the formulation of the crack interaction problem for multiple planar cracks is presented, and the method to obtain the stress field is developed. The number of cracks, their relative dimensions, orientations and locations are all variables of the present formulation. It is not possible to present the crack propagation for all of these parameters. Therefore, only some sample configurations are presented here and related crack propagation directions are determined. These parameters are chosen in such a way that gives the best insight into the effect of interaction to the propagation phenomena.

During crack propagation, the original crack geometry will change and strongly affect the fracture parameters. Since it is almost impossible to develop a model that can include all possible changes of crack geometry before hand, the process in general is carried out incrementally. Starting from a given crack shape and size, all field variables and fracture parameters can be obtained, and this would enable one to determine the possible crack growth direction(s) at a given state of stress. After determining the growth direction from the tip, the next step is to extend the crack along that direction in a small amount and re-solve the crack problem for the new configuration. This incremental process can be repeated until the crack becomes sufficiently long or grows in an unstable manner.

The main goal in this study is to determine the effect of crack–defect interaction on the initial crack propagation direction at a crack tip that is surrounded by other cracks or inclusions. In order to do that one needs to obtain the elastic stress field in the presence of multiple cracks and/or inclusions or voids. The following two sections are devoted to modeling this problem. First, a main crack interacting with multiple cracks is considered. This is followed by the interaction of a crack with an inclusion. After presenting the basic solutions for these cases, the propagation problem is addressed. The cracks are represented by dislocation density distributions and a set of coupled integral equations is derived to find these densities that are later used in the evaluation of the stress intensity factors. Shielding and amplification effects of additional cracks and nearby inclusion, depending on relative sizes, positions and orientations, are briefly mentioned. A more complete analysis of the crack–crack interaction problem is presented in [9] while the basic formulation of the crack–inclusion interaction is presented in [10]. The propagation behavior of a crack near a void and inclusion is analyzed in [11] by using five different criteria. The minimum strain energy density criterion is used in [12] to investigate the conditions under which the crack goes around or runs into the inclusion. In this study, after introducing each criterion, the crack propagation direction at the close tip of a crack near to other defects is investigated.

2. The crack–crack interaction problem

A number of finite cracks located in an infinite planar domain subjected to uniform stresses at infinity are considered. The cracks are arbitrarily located relative to each other. Each mixed mode crack is

represented by the distributions of dislocation densities composed of two components of Burgers vectors corresponding to mode I and mode II which are represented by the indices n and t, respectively. The formulation given in [9] can be repeated for M number of cracks. Applying the following boundary conditions by choosing the global coordinate system based on the center of one of the cracks (referenced as main crack)

$$\sigma_{yy} = \sigma_0, \quad \sigma_{yx} = \tau_0, \quad \sigma_{xx} = 0, \text{ at } \infty \tag{1}$$

and condition of traction free crack surfaces requires that

$$t_{n_i} = 0, \quad t_{t_i} = 0, \tag{2}$$

where t_n and t_t represent normal and tangential tractions at the surfaces of ith crack, this leads to the following set of integral equations:

$$-D\int_{-a_i}^{a_i} \frac{b_{n_i}(s_i)}{(x_i - s_i)}\,\mathrm{d}s_i = -\sigma_{0_i} + D\sum_{j=1}^{M}\int_{-a_j}^{a_j}\left[b_{n_j}(s_j)K_{ij}^{n}(s_j,x_i) + b_{t_j}(s_j)K_{ij}^{t}(s_j,x_i)\right]\mathrm{d}s_j, \tag{3}$$

$$-D\int_{-a_i}^{a_i} \frac{b_{t_i}(s_i)}{(x_i - s_i)}\,\mathrm{d}s_i = -\tau_{0_i} + D\sum_{j=1}^{M}\int_{-a_j}^{a_j}\left[b_{n_j}(s_j)L_{ij}^{n}(s_j,x_i) + b_{t_j}(s_j)L_{ij}^{t}(s_j,x_i)\right]\mathrm{d}s_j \tag{4}$$

along with the additional complementary conditions

$$\int_{-a_i}^{a_i} b_{n_i}(s_i)\,\mathrm{d}s_i = 0, \quad \int_{-a_i}^{a_i} b_{t_i}(s_i)\,\mathrm{d}s_i = 0, \tag{5}$$

where $i = 1,\ldots,M$ and $j = 1,\ldots,M$. b_n and b_t are the dislocation density distributions corresponding to the opening (mode I) and sliding (mode II) modes, respectively. The kernels K_{ij} and L_{ij} are functions of positions of crack i relative to crack j and the transformation angle of stresses. Their general form is given in [9] and [22]. Note also that a_i and a_j are the half-lengths of ith and jth cracks. σ_{0_i} and τ_{0_i} are the traction components on the positions of the crack surfaces in the flawless material due to of the external loading and are given by

$$\begin{aligned} -\sigma_{0_i} &= -\sigma_0\cos\alpha_{\mathrm{i}}^2 + \tau_0\sin 2\alpha_{\mathrm{i}}, \\ -\tau_{0_i} &= -\frac{1}{2}\sigma_0\sin 2\alpha_{\mathrm{i}} + \tau_0\cos 2\alpha_{\mathrm{i}}. \end{aligned} \tag{6}$$

where α_{i} is the inclination angle of the crack relative to the x-axis. The numerical solution of the above M-coupled integral equations by any of the available methods for singular integral equations gives the dislocation density distribution. Using these distributions, the components of the stress field at any point in the domain can be obtained by adopting the expressions of [13] as follows:

$$\sigma_{xx} = D\sum_{i=1}^{M}\left[\int_{-1}^{1} b_{yi}(s_i)\frac{x_{si}\left[x_{si}^2 - y_{si}^2\right]}{\left(x_{si}^2 + y_{si}^2\right)^2}\,\mathrm{d}s_i - \int_{-1}^{1} b_{xi}(s_i)\frac{y_{si}\left[y_{si}^2 + 3x_{si}^2\right]}{\left(x_{si}^2 + y_{si}^2\right)^2}\,\mathrm{d}s_i\right], \tag{7}$$

$$\sigma_{yy} = D\sum_{i=1}^{M}\left[\int_{-1}^{1} b_{yi}(s_i)\frac{x_{si}\left[x_{si}^2 + 3y_{si}^2\right]}{\left(x_{si}^2 + y_{si}^2\right)^2}\,\mathrm{d}s_i + \int_{-1}^{1} b_{xi}(s_i)\frac{y_{si}\left[x_{si}^2 - y_{si}^2\right]}{\left(x_{si}^2 + y_{si}^2\right)^2}\,\mathrm{d}s_i\right], \tag{8}$$

$$\sigma_{xy} = D\sum_{i=1}^{M}\left[\int_{-1}^{1} b_{yi}(s_i)\frac{y_{si}\left[y_{si}^2 - x_{si}^2\right]}{\left(x_{si}^2 + y_{si}^2\right)^2}\,\mathrm{d}s_i + \int_{-1}^{1} b_{xi}(s_i)\frac{x_{si}\left[x_{si}^2 - y_{si}^2\right]}{\left(x_{si}^2 + y_{si}^2\right)^2}\,\mathrm{d}s_i\right], \tag{9}$$

where $D = 2G/(\pi(\kappa+1))$ and $\kappa = 3\text{–}4v$ for plane strain and $\kappa = (3-v)/(1+v)$ for plane stress. $x_{si} = x_i - s_i$ and $y_{si} = y_i$, x_i and y_i are local Cartesian coordinates of a point where the stresses are calculated. b_{yi} and b_{xi} are the transformed form of the normal an tangential components of Burgers vectors.

3. The crack–inclusion/void interaction problem

The stress field in an infinite plane including a circular inclusion and a nearby crack subjected to uniaxial stresses at infinity can be obtained in two steps by applying the superposition principle. The first part is the stress field in an infinite plane with a circular inclusion subjected to a uniaxial state of stress σ_0 applied at infinity. This can be obtained using readily available solution for uniaxial stress case presented in [14] as follows:

$$\sigma_{rr} = \frac{\sigma_0}{2}\left[1 - \frac{\gamma r_0^2}{r^2} + \left(1 - \frac{2\lambda r_0^2}{r^2} - \frac{3\delta r_0^4}{r^4}\right)\cos 2\theta\right], \tag{10}$$

$$\sigma_{\theta\theta} = \frac{\sigma_0}{2}\left[1 - \frac{\gamma r_0^2}{r^2} - \left(1 - \ - \frac{3\delta r_0^4}{r^4}\right)\cos 2\theta\right], \tag{11}$$

$$\sigma_{r\theta} = -\frac{\sigma_0}{2}\left[1 + \frac{\gamma r_0^2}{r^2} + \left(1 - \frac{2\lambda r_0^2}{r^2} - \frac{3\delta r_0^2}{r^4}\right)\sin 2\theta\right], \tag{12}$$

where $\lambda = -2(G_2 - G_1)/G_1 + \kappa_1 G_2$, $\gamma = G_1(\kappa_2 - 1) - G_2(\kappa_1 - 1)/2G_2 + G_1(\kappa_2 - 1)$, $\delta = -(G_2 - G_1)/G_1 + \kappa_1 G_2$, and r_0 is the radius of the inclusion, the origin of the polar coordinates is at the center of the inclusion and θ is measured from the direction of loading axis. G_1, G_2 and κ_1, κ_2 are the elastic constants of the matrix and the inclusion, respectively. The second part is to model the crack as a pile-up of dislocations, but now the stress field used is that of an edge dislocation near an inclusion which is given in [15], but modified and written in the following form:

$$\sigma^1_{yy} = \frac{2G_1}{\pi(\kappa_1+1)}\left[b_x G^1_{xyy} + b_y G^1_{yyy}\right], \tag{13}$$

$$\sigma^1_{xx} = \frac{2G_1}{\pi(\kappa_1+1)}\left[b_x G^1_{xxx} + b_y G^1_{yxx}\right], \tag{14}$$

$$\sigma^1_{xy} = \frac{2G_1}{\pi(\kappa_1+1)}\left[b_x G^1_{xxy} + b_y G^1_{yxy}\right], \tag{15}$$

where G terms are given in [16].

The integral equations for the crack–inclusion interaction case can be written using the above expressions. Following the notation of [16] and observing that the singularities in the kernel come from the terms containing x_1/r_1^2 and y_1/r_1^2 which are given as

$$\frac{x_1}{r_1^2} = -\frac{s}{\sqrt{c^2+s^2}(s-x)}, \quad \frac{y_1}{r_1^2} = \frac{c}{\sqrt{c^2+s^2}(s-x)}, \tag{16}$$

and after separating the singular terms, the singular integral equations representing the interaction case will have the following form (see Fig. 13):

$$\int_{a_1}^{a_2} \frac{b_x(s)c}{\sqrt{c^2+s^2}(s-t)}\,\mathrm{d}s + \int_{a_1}^{a_2} K_{11}(s,t)b_x(s)\,\mathrm{d}s + \int_{a_1}^{a_2} \frac{b_y(s)c}{\sqrt{c^2+s^2}(s-t)}\,\mathrm{d}s + \int_{a_1}^{a_2} K_{12}(s,t)b_y(s)\,\mathrm{d}s = -\bar{\sigma}_{ww}, \tag{17}$$

$$\int_{a_1}^{a_2} \frac{b_x(s)s}{\sqrt{c^2+s^2}(s-t)}\,\mathrm{d}s + \int_{a_1}^{a_2} K_{21}(s,x)b_x(s)\,\mathrm{d}s + \int_{a_1}^{a_2} \frac{b_y(s)c}{\sqrt{c^2+s^2}(s-t)}\,\mathrm{d}s + \int_{a_1}^{a_2} K_{22}(s,t)b_y(s)\,\mathrm{d}s = -\bar{\sigma}_{nttw}, \tag{18}$$

where

$$\bar{\sigma}_{ww} = \frac{\pi(\kappa+1)}{2G_1}\left(\sigma^1_{xx}\cos^2\alpha + \sigma^1_{yy}\sin^2\alpha + 2\sigma^1_{xy}\sin\alpha\cos\alpha\right), \tag{19}$$

$$\bar{\sigma}_{tw} = \frac{\pi(\kappa+1)}{2G_1}\left((\sigma^1_{yy}-\sigma^1_{xx})\sin\alpha\cos\alpha + \sigma^1_{xy}(\cos^2\alpha-\sin^2\alpha)\right), \tag{20}$$

and σ^1_{xx}, σ^1_{yy} and σ^1_{xy} are the stress components obtained from the solution without crack in the first part and the kernels K_{ij} are given in Appendix A. Once the stress field from all defects is obtained, the stress intensity factors can also be computed numerically as discussed in [21].

4. Crack propagation theories

There have been numerous crack initiation and/or propagation theories proposed over the years. However, only a few of them have been proven to be viable and producing results that agree with some experimental observations. The maximum circumferential stress theory, minimum strain energy density theory and maximum strain energy release rate theory are considered to be the most important ones among these theories. The first two criteria are used in the present study. However, because of the crack-tip singularity a cut off radius from the crack tip at which the stress is calculated is also introduced. As seen in the calculations below this concept does not affect the propagation directions significantly.

4.1. Maximum circumferential stress (maximum normal stress) theory

The maximum circumferential (tangential) stress criterion proposed by Erdogan and Sih [17] is a commonly recognized hypothesis for crack extension in a brittle material under slowly applied in-plane loads. This criterion has later been derived based on the principle of minimum potential energy [18]. The theory states that the direction of crack extension is in the radial direction from the crack tip and is normal to the maximum tangential (circumferential or hoop) stress ($\sigma_{\theta\theta}$) at the original crack tip. The results of this theory are in remarkable agreement with slit cracks; however, the agreement is not so great for elliptical cracks. Since the present model is developed for slit-like cracks, it will be convenient to use this crack extension theory. Agreement in the case of elliptical cracks is also observed when higher order terms are included in the stress expressions.

Following the developments of the Westergaard stress function, formulation for a crack in an infinite plane close tip stress field for mixed mode cracks is given in the literature as follows [19]:

$$\sigma_{rr} = \frac{K_{\mathrm{I}}}{\sqrt{2\pi r}}\left(\frac{5}{4}\cos\frac{\theta}{2} - \frac{1}{4}\cos\frac{3\theta}{2}\right) + \frac{K_{\mathrm{II}}}{\sqrt{2\pi r}}\left(-\frac{5}{4}\cos\frac{\theta}{2} + \frac{3}{4}\sin\frac{3\theta}{2}\right), \tag{21}$$

$$\sigma_{\theta\theta} = \frac{K_{\mathrm{I}}}{\sqrt{2\pi r}}\left(\frac{3}{4}\cos\frac{\theta}{2} + \frac{1}{4}\cos\frac{3\theta}{2}\right) + \frac{K_{\mathrm{II}}}{\sqrt{2\pi r}}\left(-\frac{3}{4}\sin\frac{\theta}{2} - \frac{3}{4}\sin\frac{3\theta}{2}\right), \tag{22}$$

$$\sigma_{r\theta} = \frac{K_I}{\sqrt{2\pi r}}\left(\frac{1}{4}\sin\frac{\theta}{2} + \frac{1}{4}\sin\frac{3\theta}{2}\right) + \frac{K_{II}}{\sqrt{2\pi r}}\left(\frac{1}{4}\cos\frac{\theta}{2} + \frac{3}{4}\cos\frac{3\theta}{2}\right), \tag{23}$$

where r and θ are the polar coordinates measured from the crack tip.

Finding the specific radial direction θ_c which makes $\sigma_{\theta\theta}$ maximum (or $\sigma_{r\theta} = 0$) is a straightforward task and is readily available in the literature. θ_c is the angle that satisfies the following equation:

$$K_I \sin\theta_c + K_{II}(3\cos\theta_c - 1) = 0. \tag{24}$$

The only needed parameters in a single mixed mode crack or multiple cracks are the stress intensity factors. Once K_I and K_{II} are known, the possible propagation direction is obtained. It has also been observed that the θ_c direction coincides with the zero shear (principal) direction. However, all the above argument is true for very small r, i.e. very close region to the crack tip where higher order terms are dropped and stress expressions are approximate. Since the crack propagation process is analyzed right at the crack tip, the above formulation gives reasonably accurate results as long as the stress intensity factors for different situations are possible to calculate. The stress intensity factors at every crack tip, as well as extended stress field, can be calculated in the present interaction case. Therefore, this criteria is applied in both closed form, by substituting the stress intensity factors in the above expression and the numerical form by searching the maximum values of $\sigma_{\theta\theta}$ obtained from the application of distributed dislocations technique and determining corresponding directions at "a certain distance". It is found that the difference is negligible. This implies that it is reasonable, at least initially, to concentrate mainly on the calculation of the stress intensity factors that enable us to express the crack extension direction in closed form. On the other hand, the higher order terms may become more important for elliptic cracks where the numerical values of the stress can still be used. However, the present analysis is restricted to slit-like cracks.

The literature relevant to crack stability tends to interchange the maximum $\sigma_{\theta\theta}$ model and the concept of crack propagation in the direction where $\sigma_{\theta\theta}$ is principal stress. Although these two concepts may be physically similar, they represent two different conditions. It is possible to have principal directions that are not the direction of maximum circumferential stress especially at a certain distance form the crack tip. It is observed in the present multiple crack interaction case that, at the very close tip region, maximum $\sigma_{\theta\theta}$ directions are also principal directions. This criterion is applied to a static problem. When it comes to dynamic crack problems where local stress parallel to the crack is greater than that normal to the crack, this theory cannot produce accurate results.

4.2. Minimum strain energy density theory (S criterion)

The minimum strain energy density criterion, proposed by Sih [20], is based on the field strength of the local strain energy density. A detailed discussion was presented in [21]. The main hypotheses of this theory state that the crack will extend in the direction of minimum strain energy density and crack extension occurs when this minimum strain energy density factor reaches a critical value ($S_{min} = S_{cr}$). S is defined such that the $1/r$ singularity is removed from the strain energy density function and is given as follows:

$$S = r\frac{dW}{dV} = r\sigma_{ij}\varepsilon_{ij}. \tag{25}$$

Again, following the derivations related to a single crack in infinite plane, the strain energy density function could be obtained by using the approximate values of close tip stresses [20]

$$S = a_{11}K_I^2 + 2a_{12}K_IK_{II} + a_{22}K_{II}^2, \tag{26}$$

where

$$a_{11} = \frac{1}{16G\pi}[(\kappa - \cos\theta)(1 + \cos\theta)], \tag{27}$$

$$a_{12} = \frac{1}{16G\pi}\sin\theta[2\cos\theta - (\kappa - 1)], \tag{28}$$

$$a_{22} = \frac{1}{16G\pi}[(\kappa + 1)(1 - \cos\theta) + (1 + \cos\theta)(3\cos\theta - 1)]. \tag{29}$$

Using the above expressions, the polar angle (θ_0) corresponding to minimum Scan be obtained in closed form. Similar to the previous criteria, once the stress intensity factors are obtained, it is possible to use either the closed form expressions at the crack tip or to make a numerical search using the stress values at certain distance from the crack tip. The latter one is more accurate. The closed form solution reveals that the result is material parameter dependent. In the present study Poisson ratio $v = 0.3$ is used for all the calculations.

In passing it is noted that when using the maximum energy release rate criteria the results show (not reported herein) that the minimum rather than the maximum G or J produces propagation directions closer to the ones found using the two criteria reported above.

5. Results and discussions

5.1. Crack–crack interaction

5.1.1. Two cracks

Two finite parallel cracks in a plane subjected to normal stresses to the main crack line at infinity, as seen in Fig. 1, are analyzed first. The change in mode I and mode II stress intensity factors at the close tips of these cracks are investigated. The contours of mode I stress intensity factor normalized by the stress intensity factor in a single crack case are depicted in Fig. 2. Two different lengths are tried for the second crack and it is observed that the general trend is similar. Therefore, crack propagation directions are an-

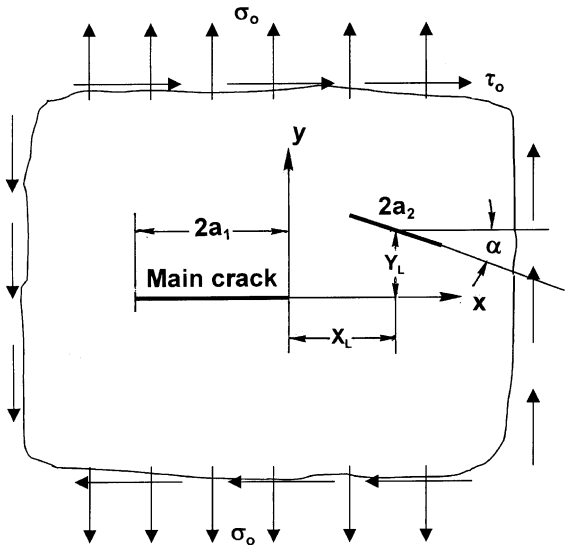

Fig. 1. Two finite crack in an infinite plane.

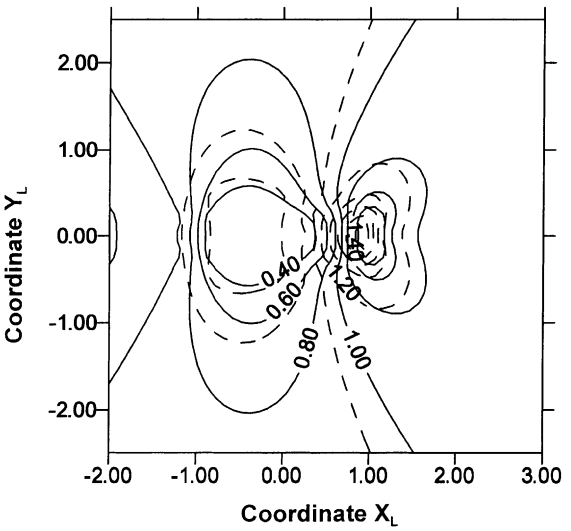

Fig. 2. The contours showing the changes in the stress intensity factors of the right tip of the main crack when the positions of another parallel crack is changed. Solid lines represent $a_2 = a_1$, dotted lines represent $a_2 = 0.1a_1$.

alyzed for the equal length cracks only. It must be noted here that X_L and Y_L are Cartesian coordinates measured from the tip of one crack to the center of the second crack and normalized by the length of the second crack. The contour line corresponding to $K_I = 1$ can be considered as a border between shielding and amplification regions and named as neutral line in the related literature. Although a slight mode II effect is observed due to interaction, it is not presented here because of its insignificant magnitude when normalized as described above.

Figs. 3 and 4 are related to the crack propagation directions at the close tip of one crack corresponding to different positions of a second crack. Fig. 3 shows the contour lines corresponding to crack propagation directions according to the maximum circumferential stress theory. The cases based on maximum circumferential stresses at a distance from the crack tip and maximum circumferential stresses coinciding with the maximum principal stress are plotted together. Fig. 4 shows crack propagation directions at the close tip according to the minimum strain energy density theory. For this specific case, the two theories agree reasonably. It can clearly be observed that crack propagation will be along the crack line in the amplifi-

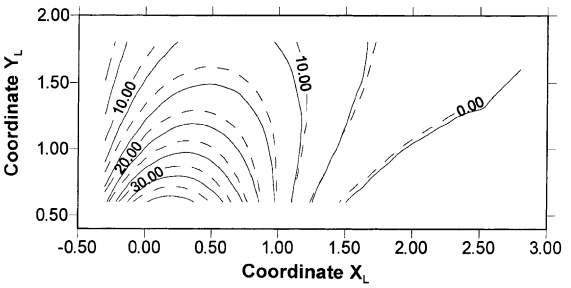

Fig. 3. Contours of crack propagation directions according to maximum circumferential stress theory. Dotted lines are the contours of the angles corresponding to the maximum value of the principal stress.

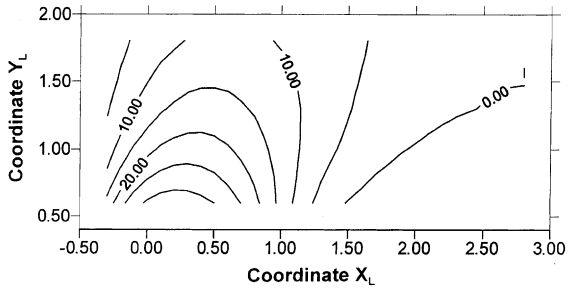

Fig. 4. Contours of crack propagation directions according to minimum strain energy density criteria.

cation region. Crack kinking is mostly expected to happen in the shielding region where mode II effect is relatively more pronounced.

In order to see the effect of changing the orientation of the neighboring crack on the crack propagation directions, Figs. 5 and 6 are plotted to show the contours of propagation directions according to the two different criteria, when the neighboring crack is rotated 30° counterclockwise. The results suggest that initial kinking will be less severe and eventually crack would propagate parallel to the crack line rather than to be pulled towards the neighboring crack. That is, the figures show smaller propagation angles in general, forcing the main crack to propagate more in self-similar manner. Further analysis showed that the rotation of the second crack loses its effect after 45° and eventually becomes ineffective at 90°.

The overall analysis shows that, depending on relative orientation, a neighboring crack will cause shielding or amplification on the close tip of the main crack. This obviously depends on its location and

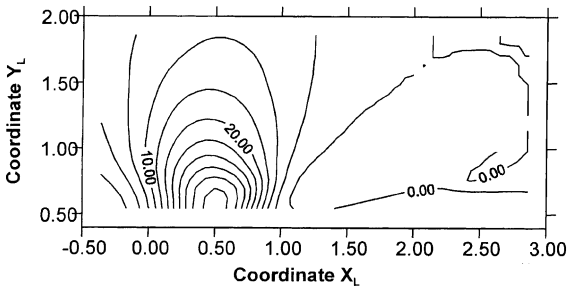

Fig. 5. Contours of crack propagation angle when the second crack is inclined 30 (maximum circumferential stress).

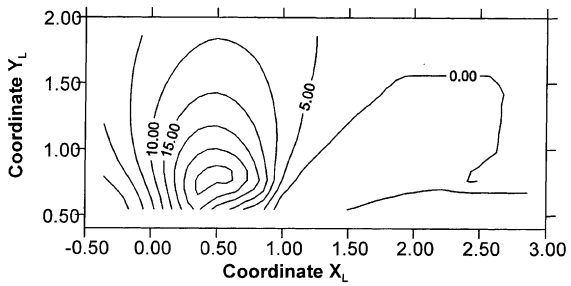

Fig. 6. Contours of crack propagation angle when the second crack is rotated 30 (minimum strain energy density).

orientation. Propagation direction will mostly stay parallel to the main crack line in the amplification case, however, when shielding is observed, the main crack is kinked towards the neighboring crack. The kinking angle is related to the amount of shielding. A decrease in mode I stress intensity factor implies a stronger mode II effect and the propagation angle increases.

5.1.2. Multiple cracks

All of the above cases were for two cracks only. When the number of neighboring cracks is increased and distributed symmetrically around the horizontal axis, they would force self-similar propagation on the main crack, which is a rather obvious conclusion. A more interesting case to analyze is the stacking of micro-cracks near the main crack tip. Fixing X_L at a certain value and putting more parallel cracks at different values of Y_L gives us the opportunity of observing the effect of an increasing number of micro-cracks (parallel stacked cracks). Table 1 shows the values of left and right stress intensity factors (K_{LI}, K_{RI}) and crack propagation directions for increasing numbers of parallel cracks at two different locations. Two characteristic values of X_L are chosen as $X_L = 0$ and $X_L = 1$, which are in shielding region and amplification region, respectively. As the table indicates, an increasing number of stacked cracks did not change the crack propagation directions and stress intensity factors significantly. However, shielding and amplification effects and distinct propagation directions in these two cases are clearly observable. Increasing the number of neighboring cracks does not affect the main crack as long as they are symmetrically distributed along the main crack line. When the symmetry is disturbed, kinking would start.

The present method is capable of analyzing randomly distributed cracks as well. Hence, using a random crack generation model, similar to that discussed in [22], the effect of randomly generated micro-cracks ahead of a main crack tip is analyzed. It is assumed that micro-cracks would nucleate ahead of a main crack along grain boundaries that are represented by pre-assigned random orientations. The average crack length assigned to a potential micro-crack represents the average length of a grain boundary. This length is assumed to be 100 times smaller than the main crack length. The effect of randomly generated micro-cracks on initial crack propagation direction is given in Fig. 7. The number of generated micro-cracks is determined at each load increment. As seen in the graph it is impossible to reach a meaningful conclusion in this case. Depending on the number, positions and orientations of the nucleated micro-cracks, the propagation direction would change. Different sets of randomly distributed micro-cracks produced similar effects and, therefore, only one case is presented here. As shown above, the effect of the closer crack dominates in general and the rest do not change that effect significantly. It is also shown that the three propagation criteria produce very similar results when applied to the present case.

5.2. Crack–inclusion/void interaction

In this section, the crack propagation directions for a crack near a void or an inclusion are analyzed. Although the subject is analyzed to some extent in some previous studies [10,11], the propagation behavior of a crack near an inclusion must be examined in order to make the analysis complete and put all interaction cases into a perspective. The formulation presented in the above section is for a general inclusion.

Table 1
The effect of parallel crack stacking on the stress intensity factors and propagation angle

X_L	0				1			
M	1	2	3	4	1	2	3	4
K_{RI}	0.454	0.457	0.453	0.448	1.389	1.348	1.333	1.323
K_{LI}	1.177	1.182	1.177	1.168	1.169	1.182	1.188	1.189
θ_c (deg)	36	36	36	36	14	14	16	16

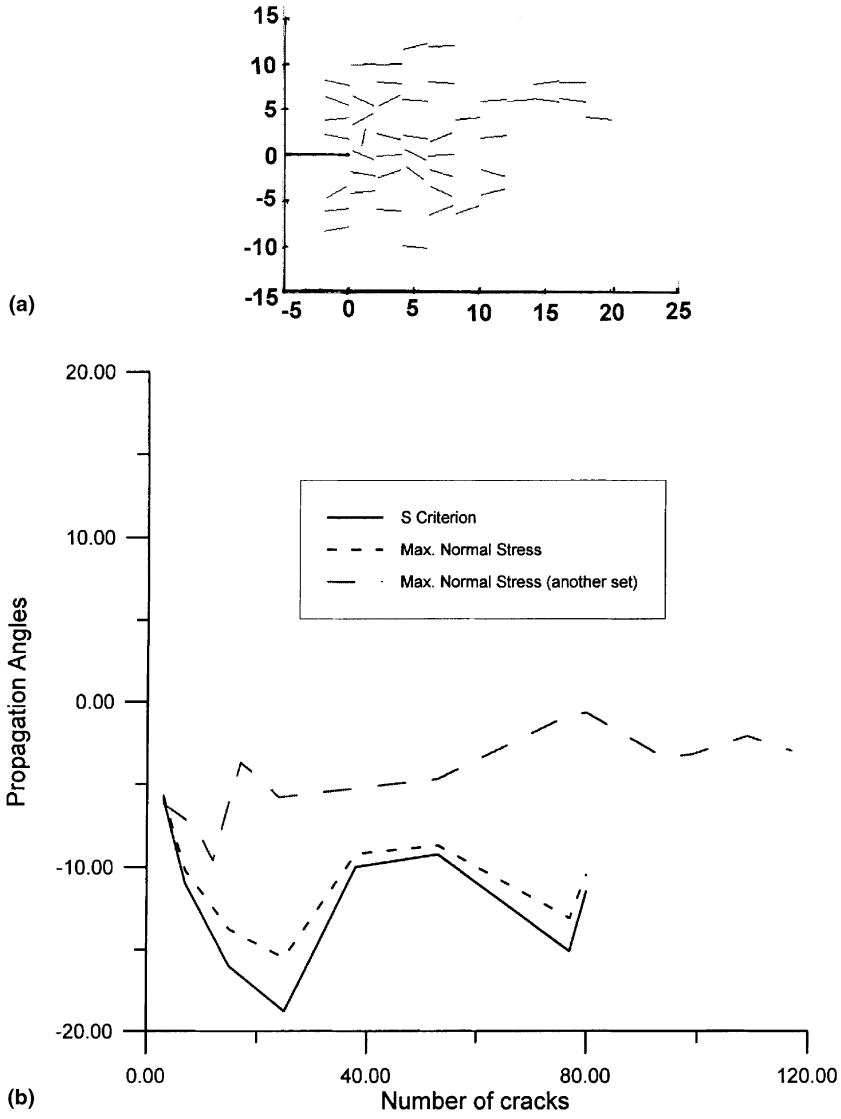

Fig. 7. (a) Randomly oriented microcracks ahead of a main crack. (b) Initial crack propagation directions at the main crack tip versus number of randomly generated microcracks.

The limiting cases of an elastic inclusion will be a hole representing void and a rigid inclusion. These limiting cases obviously correspond to setting the shear modulus of the inclusion equal to zero and infinity, respectively. The present model calculates stress intensity factors as well as extended the stress field in the case of crack–inclusion interaction. The values of the stress intensity factor are used to find the initial crack propagation directions. The contours of propagation directions at the close tip of a horizontal crack (i.e. the loading is perpendicular to the crack) near a hole are plotted in Figs. 8 and 9 for the two criteria used in the present study. Here "close tip" refers to the crack tip that is closer to the inclusion. The XT and YT coordinates show the positions of the close tip of the crack. The different criteria give slightly different results however the general trend is similar. The general trend is that the crack is pulled towards the hole as expected.

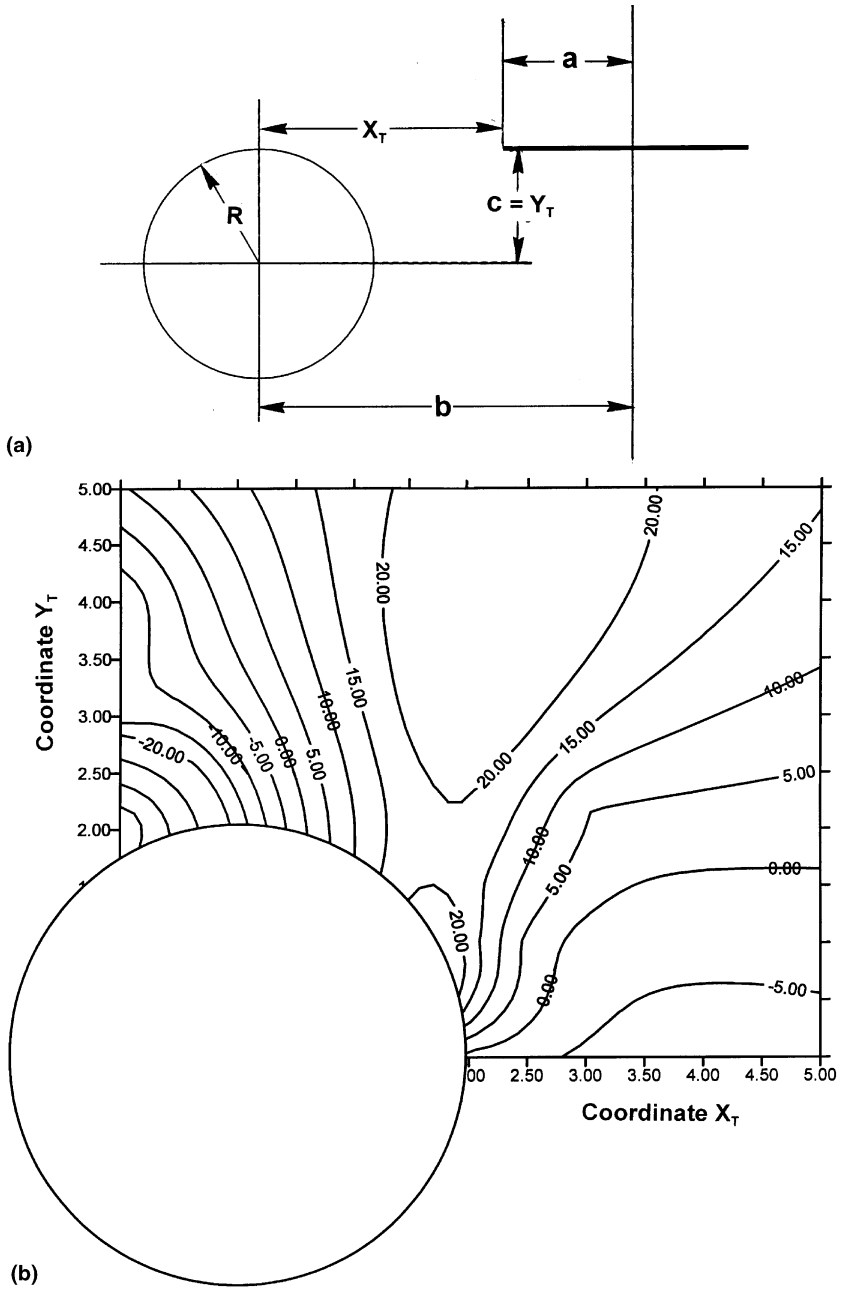

Fig. 8. (a) Parameters for the inclusion crack interaction problem. (b) The contours of initial crack propagation directions versus the position of the close tip of a horizontal crack around a hole according to maximum circumferential stress theory.

Figs. 10 and 11 show the same contours around a rigid inclusion. The inclusion is modeled in the numerical calculations by setting the ratio of the shear modulus of the inclusion and matrix $\mu_2/\mu_1 = 23$ and $\kappa_1 = 1.6$ for the matrix and $\kappa_2 = 1.8$ for the inclusion. These values are selected to make the results comparable to those given in [9,10]. It can be deduced from the figures that the general effect of the

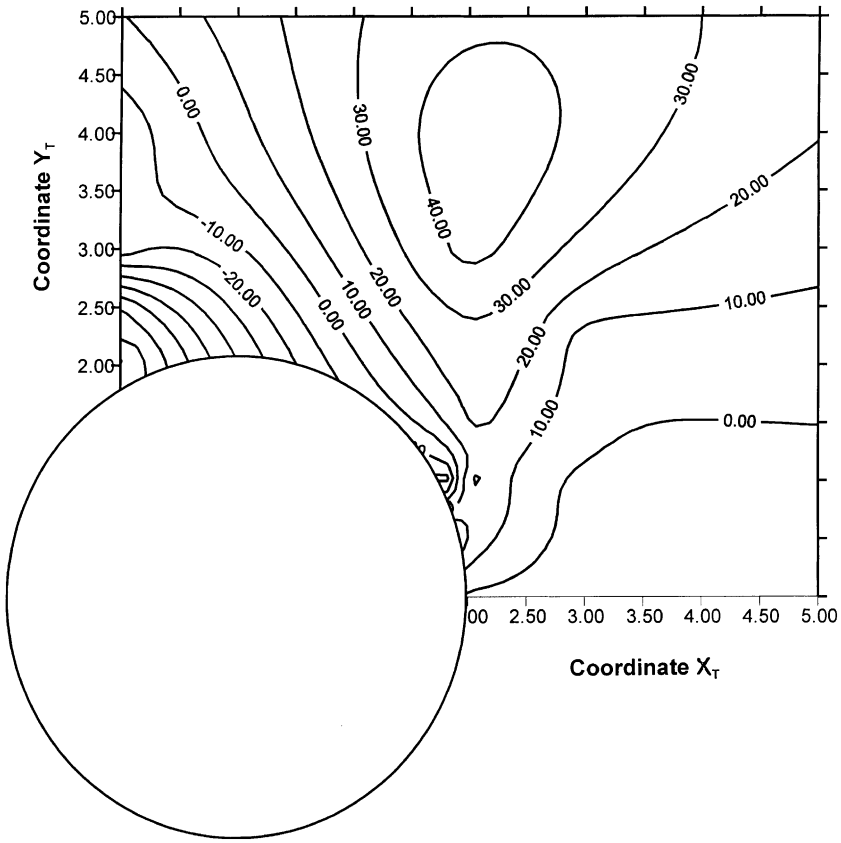

Fig. 9. The contours of initial crack propagation directions versus the position of the close tip of a horizontal crack around a hole according to minimum strain energy density theory (*S* criterion).

inclusion is to push the crack away except in the region along the centerline of the inclusion. In that region the stress intensity factor is significantly amplified and mode II is negligible.

In conclusion, a general framework based on the theory of dislocation pile-up to investigate crack propagation under mixed modes and in the presence of various other defects, micro-cracks, voids and or inclusions has been developed. It is shown that the type of defect(s) and their location near the crack tip have significant influence on crack initiation, propagation direction, and kinking. The numerical framework developed here can be employed to investigate problems involving large numbers of defects of the types considered in the present study. The present study lays the foundation of an extensive analysis of crack propagation, coalescence and failure path and form prediction. Addition of the formulation of the kinked crack solution is the step that could link this study to the next stage. An incremental analysis is needed to follow the entire crack propagation path.

Acknowledgements

The support of the US National Science Foundation under grant number CMS-9634726 to Zbib, and the partial support of the Pacific Northwest National Laboratory to Demir during the summers of 1999 and

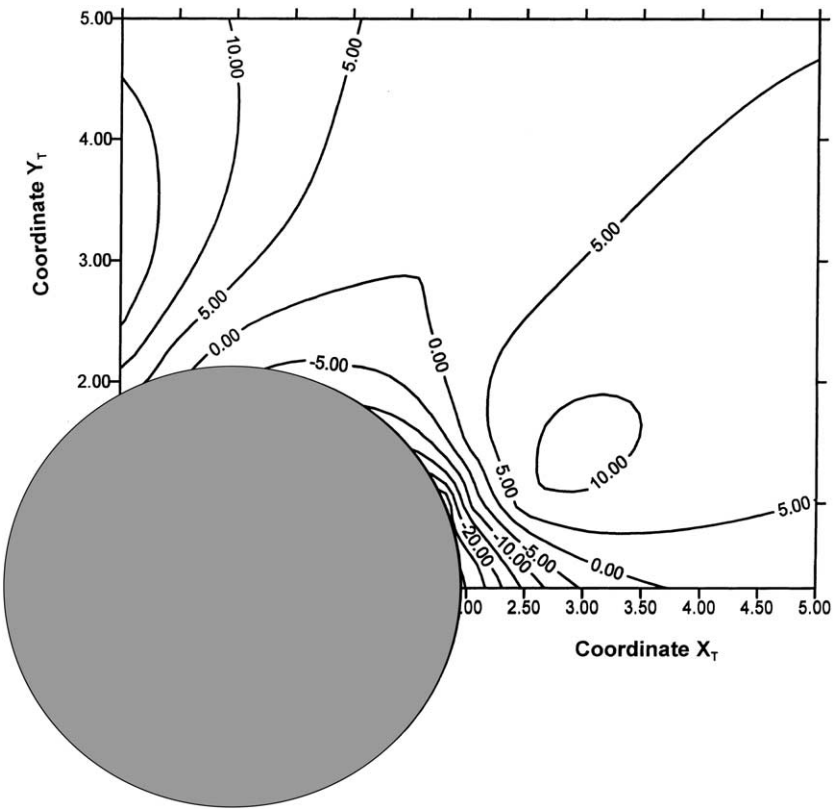

Fig. 10. The contours of initial crack propagation directions versus the position of the close tip of a horizontal crack around a rigid inclusion according to maximum circumferential stress theory.

2000, and support by King Saud University College of Engineering Research Center are gratefully acknowledged.

Appendix A

The kernels of the integral equations (17) and (18) for the crack inclusion interaction case are (see Figs. 12 and 13):

$$K_{11} = F_{xxx}\cos^2\alpha + F_{xyy}\sin^2\alpha + 2F_{xxy}\sin\alpha\cos\alpha,$$

$$K_{12} = F_{yxx}\cos^2\alpha + F_{yyy}\sin^2\alpha + 2F_{yxy}\sin\alpha\cos\alpha,$$

$$K_{21} = (F_{xyy} - F_{xxx})\sin\alpha\cos\alpha + F_{xxy}(\cos^2\alpha - \sin^2\alpha),$$

$$K_{22} = (F_{yyy} - F_{yxx})\sin\alpha\cos\alpha + F_{yxy}(\cos^2\alpha - \sin^2\alpha),$$

with (see also [13])

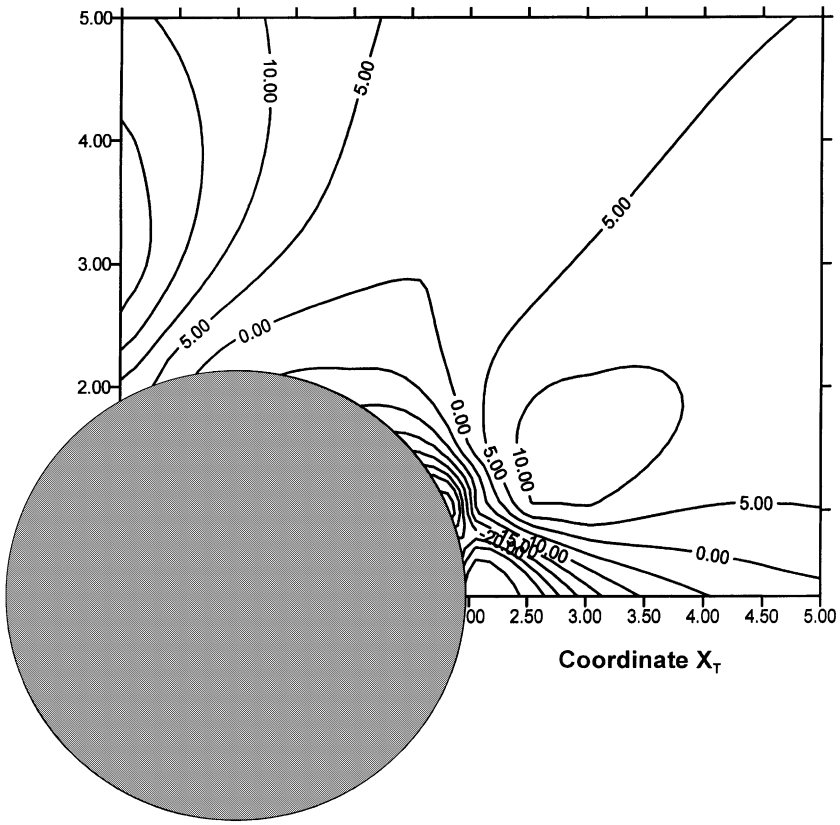

Fig. 11. The contours of initial crack propagation directions versus the position of the close tip of a horizontal crack around a rigid inclusion according to minimum strain energy density theory (S criterion).

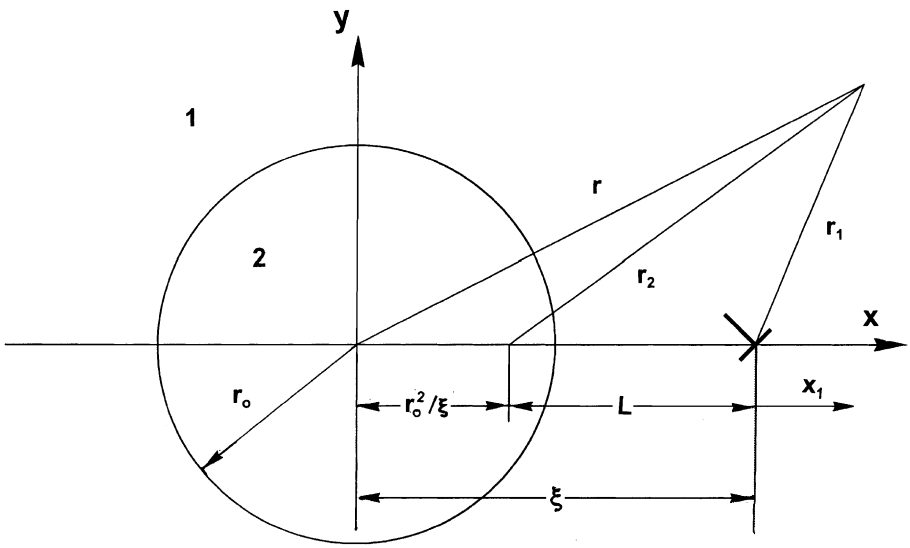

Fig. 12. Dislocation near a void or inclusion.

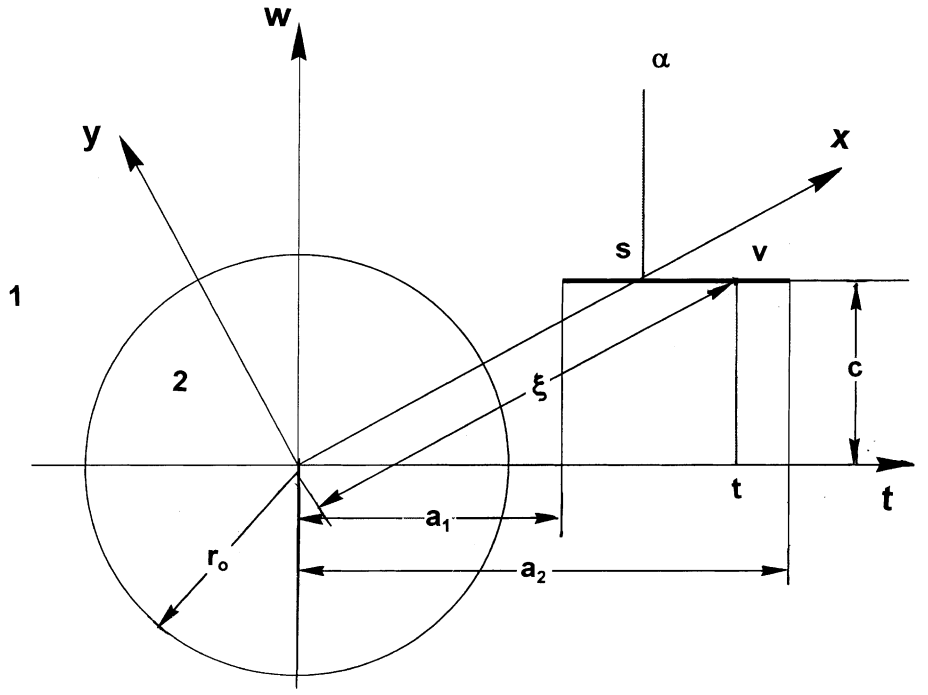

Fig. 13. Crack near a void or inclusion.

$$
\begin{aligned}
F_{xyy} = & -\frac{y}{r_2^2}\left[\frac{2Ax_2^2}{r_2^2}+\frac{B-3A}{2}\right]+\frac{y}{r^2}\left[\frac{2Ax^2}{r^2}+\frac{B-3A}{2}\right]+\frac{2AyL}{r_2^4d^2}\left[\frac{4x_2^2}{r_2^2}\left(\frac{L}{2}-x_2\right)+\left(3x_2-\frac{L}{2}\right)\right]\\
& -\frac{r_0y}{r^4}\left[r_0A\left(\frac{4x^2}{r^2}-1\right)+\frac{x}{d}(A-B)\right],\\
F_{yyy} = & \frac{x_2}{r_2^2}\left[\frac{2Ax_2^2}{r_2^2}-\frac{B+5A}{2}\right]-\frac{x}{r^2}\left[\frac{2Ax^2}{r^2}-\frac{B+5A}{2}\right]+\frac{2Ax_2L}{r_2^4d^2}\left[\frac{4x_2^2}{r_2^2}\left(\frac{L}{2}-x_2\right)+\left((5-d^2)x_2-\frac{3L}{2}\right)\right]\\
& +\frac{r_0x}{r^4}\left[r_0A\left(\frac{4x^2}{r^2}-3\right)+\frac{x}{d}(A(2d^2-1)+Q-1)\right]-\frac{r_0[A(2d^2-1)+Q-1]}{2r^2d}-\frac{AL}{r_2^2}\left[\frac{2}{d^2}-1\right],\\
F_{xxx} = & \frac{y}{r_2^2}\left[\frac{2Ax_2^2}{r_2^2}+\frac{B+A}{2}\right]-\frac{y}{r^2}\left[\frac{2Ax^2}{r^2}+\frac{B+A}{2}\right]-\frac{2AyL}{r_2^4d^2}\left[\frac{4x_2^2}{r_2^2}\left(\frac{L}{2}-x_2\right)+\left(x_2-\frac{L}{2}\right)\right]\\
& +\frac{r_0y}{r^4}\left[r_0A\left(\frac{4x^2}{r^2}-1\right)+\frac{x}{d}(A-B)\right],\\
F_{yxx} = & -\frac{x_2}{r_2^2}\left[\frac{2Ax_2^2}{r_2^2}-\frac{B+A}{2}\right]+\frac{x}{r^2}\left[\frac{2Ax^2}{r^2}-\frac{B+A}{2}\right]-\frac{2Ax_2L}{r_2^4d^2}\left[\frac{4x_2^2}{r_2^2}\left(\frac{L}{2}-x_2\right)+\left((3-d^2)x_2-3\frac{L}{2}\right)\right]\\
& -\frac{r_0x}{r^4}\left[r_0A\left(\frac{4x^2}{r^2}-3\right)+\frac{x}{d}\left(A(2d^2-1)+Q-1\right)\right]+\frac{r_0[A(2d^2-1)+Q-1]}{2r^2d}-\frac{AL}{r_2^2},\\
F_{xxy} = & -\frac{x_2}{r_2^2}\left[\frac{2Ax_2^2}{r_2^2}+\frac{B-3A}{2}\right]+\frac{x}{r^2}\left[\frac{2Ax^2}{r^2}+\frac{B-3A}{2}\right]+\frac{2Ax_2L}{r_2^4d^2}\left[\frac{4x_2^2}{r_2^2}\left(\frac{L}{2}-x_2\right)+\left(4x_2-3\frac{L}{2}\right)\right]\\
& -\frac{r_0x}{r^4}\left[r_0A\left(\frac{4x^2}{r^2}-3\right)+\frac{x}{d}(A-B)\right]-\frac{AL}{r_2^2d^2}+\frac{r_0(A-B)}{2r^2d},
\end{aligned}
$$

$$F_{yxy} = -\frac{y}{r_2^2}\left[\frac{2Ax_2^2}{r_2^2} - \frac{B+A}{2}\right] + \frac{y}{r^2}\left[\frac{2Ax^2}{r^2} - \frac{B+A}{2}\right] - \frac{2AyL}{r_2^4 d^2}\left[\frac{4x_2^2}{r_2^2}\left(\frac{L}{2} - x_2\right) + \left((2-d^2)x_2 - \frac{L}{2}\right)\right] - \frac{r_0 y}{r^4}\left[r_0 A\left(\frac{4x^2}{r^2} - 1\right) + \frac{x}{d}\left(A(2d^2-1) + Q - 1\right)\right],$$

where

$$d = \frac{\xi}{r_0}, \quad L = \frac{r_0(d^2-1)}{d}, \quad x_1 = x - \xi, \quad x_2 = x_1 + L,$$
$$r^2 = x^2 + y^2, \quad r_1^2 = x_1^2 + y^2, \quad r_2^2 = x_2^2 + y^2,$$
$$\cos\alpha = \frac{c}{\sqrt{s^2+c^2}}, \quad \sin\alpha = \frac{s}{\sqrt{s^2+c^2}},$$
$$x = t\sin\alpha + c\cos\alpha, \quad y = c\sin\alpha - t\cos\alpha,$$
$$x_1 = \frac{s(t-s)}{\sqrt{s^2+c^2}}, \quad x_2 = \frac{ts + c^2 - r_0^2}{\sqrt{s^2+c^2}},$$
$$r = c^2 + t^2, \quad r_1^2 = (s-t)^2, \quad r_2^2 = \frac{(st + c^2 - r_0^2)^2 + c^2(s-t)^2}{c^2+s^2},$$
$$d = \frac{\xi}{r_0}, \quad L = \frac{r_0(d^2-1)}{d},$$
$$A = \frac{\beta - \alpha}{1+\beta}, \quad B = -\frac{\alpha+\beta}{1-\beta}, \quad Q = \frac{(1+\alpha)(1-\alpha)}{(1-\beta)(1+\alpha-2\beta)},$$

where α and β are Dundurs parameters that are defined as:

$$\alpha = \frac{G_2(\kappa_1+1) - G_1(\kappa_2+1)}{G_2(\kappa_1+1) + G_1(\kappa_2+1)}, \quad \beta = \frac{G_2(\kappa_1-1) - G_1(\kappa_2-1)}{G_2(\kappa_1+1) + G_1(\kappa_2+1)}.$$

References

[1] B. Cotterell, J.R. Rice, Slightly curved or kinked cracks, Int. J. Fract. 16 (1980) 155–161.
[2] K.K. Lo, Analysis of branched cracks, J. Appl. Mech. 45 (1978) 797–805.
[3] S. Nemat-Nasser, L.M. Keer, K.S. Parihar, Unstable growth of thermally induced interacting cracks in brittle solids, Int. J. Solids Struct. 14 (1978) 409–430.
[4] K. Hayashi, S. Nemat-Nasser, Energy release rate and crack kinking, Int. J. Solids Struct. 17 (1981) 7–18.
[5] H. Gao, C. Chiu, Slightly curved or kinked cracks in anisotropic elastic solids, Int. J. Solids Struct. 29 (1992) 947–955.
[6] M. Hori, N. Vaikuntan, Rigorous formulation of crack path in two-dimensional elastic body, Mech. Mater. 26 (1) (1997) 1–14.
[7] H. Strifors, A generalized force measure of conditions at crack tips, Int. J. Solids Struct. 10 (1974) 1389–1404.
[8] G.C. Sih, J.Z. Zhuo, Multiscale behavior of crack initiation and growth in piezoelectric ceramics, J. Theor. Appl. Fract. Mech. 34 (2) (2000) 123–141.
[9] I. Demir, Interaction between finite planar cracks, King Saud Univ. J. (Eng. Sci.) 11 (1) (1999) 85–116.
[10] F. Erdogan, G.D. Gupta, M. Ratwani, Interaction between a circular inclusion and an arbitrarily oriented crack, J. Appl. Mech. 41 (4) (1974) 1007–1011.
[11] C.-F. Sheng, L. Wheeler, Crack path prediction for a kinked crack in the neighborhood of a circular inclusion in an infinite medium, J. Appl. Mech. 48 (2) (1981) 313–319.
[12] C.K. Chao, Stability of crack interacting with fibers, in: G.C. Sih, S.E. Hsu (Eds.), Advanced Composite Materials and Structures, XNU Science Press, The Netherlands, 1986, pp. 365–374.
[13] J.P. Hirth, J. Lothe, Theory of Dislocations, second ed., Wiley, New York, 1982.

[14] N.I. Muskhelishvili, Some Basic Problems in the Mathematical theory of Elasticity, Nordhoff, Groningen, Holland, 1953.
[15] J. Dundurs, T. Mura, Interaction between an edge dislocation and a circular inclusion, J. Mech. Phys. Solids 12 (1964) 177–189.
[16] D.A. Hills, P.A. Kelly, D.N. Dai, A.M. Korsunsky, Solution of Crack Problems: The Distributed Dislocation Technique, Kluwer Academic Publishers, The Netherlands, 1996.
[17] F. Erdogan, G.C. Sih, On the crack extension in plates under plane loading and transverse shear, Trans. ASME, J. Basic Eng. 85 (1963) 519–527.
[18] M. Shen, M.H. Sehn, direction of crack extension under general plane loading, Int. J. Fract. 70 (1995) 51–58.
[19] T.L. Anderson, Fracture Mechanics: Fundamentals and Applications, CRC Press, Boca Raton, FL, 1995.
[20] G.C. Sih, A special theory of crack propagation, in: G.C. Sih (Ed.), Methods of Analysis and Solutions of Crack Problems, vol. 1, Martinus Nijhoff, The Netherlands, 1973.
[21] G.C. Sih, Mechanics of Fracture Initiation and Propagation, Kluwer Academic Publishers, Dordrecht, 1991.
[22] I. Demir, H.M. Zbib, A mesoscopic model for inelastic deformation and damage, Int. J. Eng. Sci., accepted.